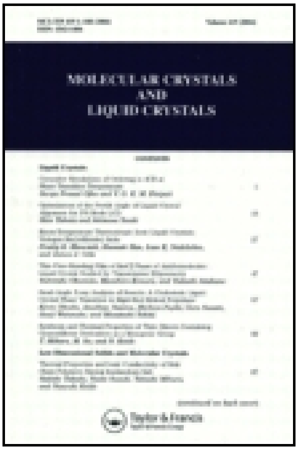

Molecular Crystals and Liquid Crystals
Publication details, including instructions for authors and subscription information:
http://www.tandfonline.com/loi/gmcl20

A.C. impedance spectrum analysis of the intercalation mechanism in hcooh-gic formation

Feiyu Kang [a] , Dongxing Yang [a] & Xinping Qiu [a]
[a] Department of Materials and Science Engineering, Tsinghua University, Beijing, 100084, China

Version of record first published: 18 Oct 2010

To cite this article: Feiyu Kang, Dongxing Yang & Xinping Qiu (2002): A.C. impedance spectrum analysis of the intercalation mechanism in hcooh-gic formation, Molecular Crystals and Liquid Crystals, 388:1, 9-14

To link to this article: http://dx.doi.org/10.1080/10587250215271

Mol. Cryst. Liq. Cryst., Vol. 388, pp. [423]/9–[428]/14
Copyright © 2002 Taylor & Francis
1058-725X/02 \$12.00 + .00
DOI: 10.1080/10587250290113781

A.C. IMPEDANCE SPECTRUM ANALYSIS OF THE INTERCALATION MECHANISM IN HCOOH-GIC FORMATION

Feiyu Kang, Dongxing Yang, and Xinping Qiu
Department of Materials and Science Engineering,
Tsinghua University, Beijing 100084, China

A.c. impedance spectroscopy was used to analyze the electrochemical intercalation of formic acid (HCOOH) into graphite. The results show that the formic acid intercalation reaction is just a process of charge transfer, adsorption and diffusion of intercalate.

Keywords: GIC; electrochemical intercalation; a.c. impedance

INTRODUCTION

Sulfuric acid and nitric acid are conventionally used in the industrial production of graphite intercalation compounds (GICs). There are two major problems. One is the release of toxic gases such as SO_x and NO_x during production. Another is the corrosion of the product during service. Therefore, the search for organic substitutes for these acids has generated much interest. Recently, we successfully synthesized HCOOH-GIC through an electrochemical method [1]. This work investigated the reaction mechanism during intercalation using a.c. impedance spectroscopy, a very useful technique for analyzing the electrochemical process of carbonaceous materials [2–6].

THEORETICAL MODEL

Generally, the physical processes taking place in an electrolytic cell can be represented by an equivalent circuit. However, the circuits are seldom unique. Figure 1(a) shows an ideal electrical model, also known as the

We are grateful for the financial support from the National Natural Science Foundation of China under Grant No.59872017.

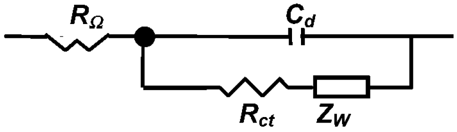

(a) Classical Randles' model

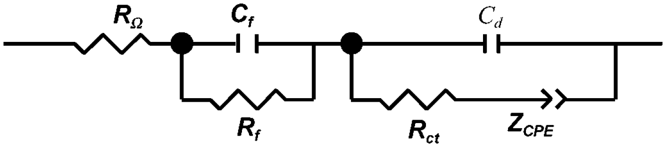

(b) Constant phase element model

FIGURE 1 Equivalent circuits used for analyzing impedance data.

Randles' model, which consists of the solution resistance R_Ω in series with a parallel connection of the double-layer capacitance C_d and faradic impedance Z_f. The parallel connection means that one part of the electrical current is used for electrode reaction and the other for the capacitance charge. Faradic impedance may be divided into charge-transfer resistance R_{ct} in series with Warburg impedance Z_w. The ideal plot in the complex plane is a standard semicircle plus a line. Usually, Randles' model works well only for smooth liquid electrodes such as mercury whereas the non-homogenous surface of solid electrodes causes deformation of the complex plane plots. The constant-phase element (CPE) model was therefore proposed for cases where a depressed semicircle was observed in complex plane plots. The semicircle was rotated by a constant phase angle $90°(1-\phi)$, where ϕ is a rotation parameter. In this case, the double-layer capacitance should be replaced by the constant-phase element (Fig. 1(b)). From Figure 1, the following equations may be obtained [6–8]:

$$
\begin{aligned}
\mathrm{Z} \equiv \mathrm{Z}' - \mathrm{j}\mathrm{Z}'' = \mathrm{R}_\Omega &+ \frac{R_{ct} + (\sigma/\sqrt{\omega})}{(1 + C_d\sigma\sqrt{\omega})^2 + \omega^2 C_d^2[R_{ct} + (\sigma\sqrt{\omega})]^2} \\
&- j\frac{\frac{\sigma}{\sqrt{\omega}}(1 + C_d\sigma\sqrt{\omega})^2 + \omega C_d[R_{ct} + (\sigma\sqrt{\omega})]^2}{(1 + C_d\sigma\sqrt{\omega})^2 + \omega^2 C_d^2[R_{ct} + (\sigma\sqrt{\omega})]^2},
\end{aligned}
$$

where R_Ω is the solution resistance, R_{ct} is the charge transfer resistance, C_d is the double-layer capacitance, j is equal to $(-1)^{1/2}$ and σ is a constant determined by electrochemical system. When $\omega \to 0$, the total resistance, Z shows linear behavior in the complex plane with an angle of 45° to the real axis, which indicates that the item relating to frequency comes from

Warburg impedance. In this case, the system is under diffusion control when the charge transfer at the electrode/electrolyte interface is much faster than the diffusion of the electrolyte ions. When $\omega \rightarrow \infty$, the plot is a characteristic semicircle, which means that the electrochemical system is controlled by electrochemical charge transfer at the electrode/electrolyte interface.

EXPERIMENTAL

Natural graphite (NG) with 99.9 wt% carbon content and highly oriented pyrolytic graphite (HOPG) was adopted as the host graphite. NG flakes with diameter of 0.3 mm was compressed to a disk of 1.15 cm in diameter. HOPG was cut into a shape of $10 \times 6 \times 0.4\,\text{mm}^3$. Reacting graphite samples served as the working electrode. Two platinum plates acted as the counter electrodes. Hg/Hg_2SO_4 electrode served as the reference electrode. 100 ml of pure formic acid ($98 \sim 100$ wt%) was used as the electrolyte and the intercalant in the electrochemical process.

A.c. impedance measurements were carried out for HOPG pieces and NG disks using a computerized potentiostat (Solarton SI1287,1255B). To stabilize the reaction system, all electrodes were polarized under a cathodic current density of $10\,\text{mA}\,\text{cm}^{-2}$ and graphite was immersed into formic acid for one night before the measurements. All the experiments were performed at room temperature. Constant potentials of 1.0, 1.2, 1.4, 1.6 and 1.8 V were maintained and kept until the residual current was smaller than 1 μA prior to the test. The impedance of the electrode/electrolyte interface was then measured by applying a sine wave of 5 mV rms amplitude over the frequency range of 100 KHz to 0.01 Hz. The measured data were analyzed using a non-linear least-square fitting program.

RESULTS AND DISCUSSION

Figure 2 shows a.c. impedance spectra of HOPG reacting with formic acid under different potentials. When the potential equaled 1.0 V, a line approaching an angle of 90° to the Z'-axis was obtained, which is the impedance spectrum typical of a blocking electrode. It indicates that detectable formic acid intercalation does not occur. As the applied potential gradually increases, the angle between the linear line and the Z'-axis decreases correspondingly. This implies that the charge transfer at the electrode/electrolyte interface becomes easier as applied potential increases. When the potential approached 1.4 V, a depressed semicircle and an inclined line is observed, as shown in Figure 2, which indicates that formic acid is intercalated into graphite layers. The depressed semicircle in

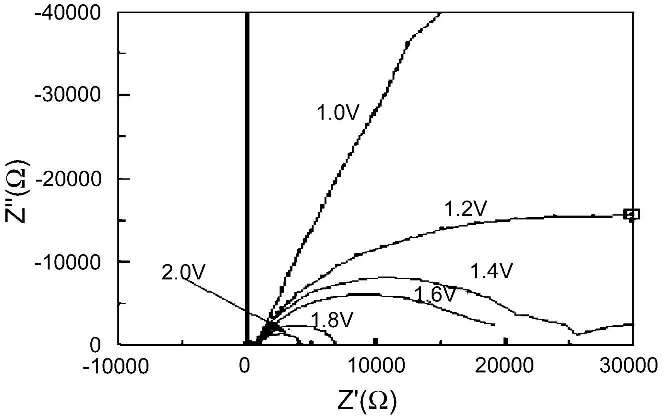

FIGURE 2 A.c. impedance spectra of HOPG in HCOOH at different potentials.

the frequency range of 1 to 10^5 Hz and the inclined line at lower frequency below 1 Hz are due to the impedance of charge transfer at the graphite/electrolyte interface and formic acid diffusion within the graphite, respectively. Figure 3 shows the a.c. impedance spectra of NG in the formic acid. The trend is similar to that of HOPG in formic acid, and the potential driving the intercalation was between 1.0 V and 1.2 V which is lower than that of HOPG (1.4 V). Thus, it is much easier for formic acid to intercalate into natural graphite than into HOPG.

Randles' circuit, as shown in Figure 1(a), is used to fit the measured impedance data. According to theory, the diameter of the semicircle

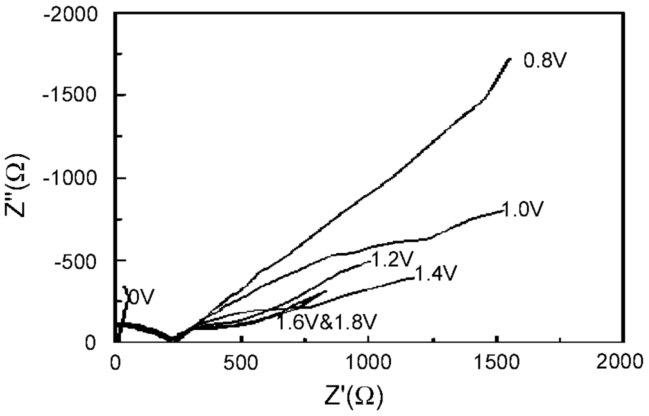

FIGURE 3 A.c. impedance spectra of NG in HCOOH at different potentials.

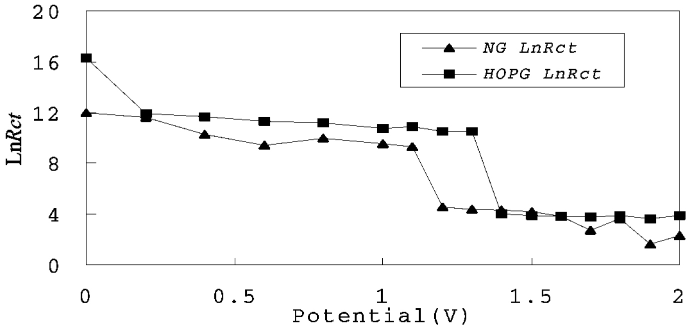

FIGURE 4 Plot of Ln(R_{ct}) *vs* applied potential of NG and HOPG in HCOOH.

represents the charge transfer resistance R_{ct}. Figure 4 shows the variation of the logarithm of the charge transfer resistance R_{ct} with electrode potential. When the applied potential is lower than the critical value, R_{ct} decreases slowly as the potential increases, and it keeps so large that intercalation does not occur. When the potential is higher than the critical value, R_{ct} decreases several orders in magnitude and the formic acid molecules can be inserted into graphite. If the potential increases continuously, intercalation may be speeded up and low stage formic acid-GIC can be formed [5]. However, R_{ct} remains almost unchanged with the increases of the electrode potential. It indicates that the stage structure of formic acid-GIC is determined by the charging time rather than potential.

According to the a.c. impedance analysis and the results from the CV curves [1], the steps in the process of formic acid intercalation can be summarized as follows: 1) Diffusion of the reactant anion $HCOO^-$ to the reaction site (graphite electrode); 2) adsorption of $HCOO^-$ or interface chemical reaction; and finally 3) charge transfer from $HCOO^-$ to graphite and diffusion in graphite layers. Stage transformation is associated with both further insertion of formic acid molecules and their rearrangement in graphite galleries until the saturation of intercalation.

CONCLUSIONS

A.c. impedance spectroscopy has been successfully used to characterize the electrochemical behavior of the intercalation of formic acid into graphite. The results show that the formic acid intercalation process is just a process of charge transfer, adsorption and diffusion of intercalate. The charge-transfer resistance changes abruptly only when electrode potential approaches the driving potential. It can be concluded that the crucial factors dominating the intercalation are the properties of the electrode/electrolyte interface.

REFERENCES

[1] Kang, F., Leng, Y., & Zhang, T.-Y. (1997). *Carbon*, *35*, 1089.
[2] Morita, M., Nishimurta, N., & Matsuda, Y. (1993). *Electrochim. Acta.*, *38*, 1721.
[3] Takami, N., Satoh, A., Hara, M., & Ohsaki, T. (1995). *J. Electrochem. Soc.*, *142*, 371.
[4] Liu, P. & Wu, P. (1995). *J. Power Sources*, *56*, 81.
[5] Funabiki, A., Inaba, M., & Ogumi, Z. (1997). *J. Power Sources*, *68*, 227.
[6] Fournier, J., Miousse, D., & Brossard, L. (1995). *Mate. Chem. Phy.*, *42*, 181.
[7] Rudolf, H. (1988). *J. Applied Electrochemistry*, *18*, 679.
[8] Liebenow, C., Wagner, M., & Luhder, K. (1995). *J. Power Sources*, *54*, 369.